Available online at www.sciencedirect.com
SCIENCE DIRECT®
Biochemical and Biophysical Research Communications 338 (2005) 318–324
BBRC
www.elsevier.com/locate/ybbrc

Generation and characterization of a transgenic mouse model with hepatic expression of human CYP2A6

Qing-Yu Zhang, Jun Gu, Ting Su, Huadong Cui, Xiuling Zhang, Jaime D'Agostino, Xiaoliang Zhuo, Weizhu Yang, Pamela J. Swiatek [1], Xinxin Ding *

Wadsworth Center, New York State Department of Health, School of Public Health, State University of New York at Albany, NY 12201, USA

Received 9 August 2005
Available online 22 August 2005

Abstract

The aim of this study was to prepare and characterize a transgenic mouse model in which CYP2A6, a human P450 enzyme, is expressed specifically in the liver. CYP2A6, which is mainly expressed in human liver, is active toward many xenobiotics. Our transgene construct contained the mouse transthyretin promoter/enhancer, a full-length CYP2A6 cDNA, and a downstream neomycin-resistance gene for positive selection in embryonic stem cells. Hepatic expression of the *CYP2A6* transgene was demonstrated by immunoblotting, whereas tissue specificity of CYP2A6 expression was confirmed by RNA-PCR. The transgenic mouse was further characterized after being backcrossed to the B6 strain for six generations. Hepatic microsomes from homozygous transgenic mice had activities significantly higher than those of B6 mice toward coumarin. The in vivo activity of transgenic CYP2A6 was also determined. Systemic clearance of coumarin was significantly higher in the transgenic mice than in B6 controls, consistent with the predicted role of CYP2A6 as the major coumarin hydroxylase in human liver. The CYP2A6-transgenic mouse model should be valuable for studying the in vivo function of this polymorphic human enzyme in drug metabolism and chemical toxicity.

Keywords: CYP2A5; CYP2A6; Transgenic mouse; Coumarin metabolism; Liver microsomes; Human P450

CYP2A6 accounts for 1–10% of total P450 in human liver [1,2]. Besides its well-known enzyme activities as a coumarin 7-hydroxylase [3] and a nicotine *C*-oxidase [4,5] in human liver microsomes, CYP2A6 is active in the metabolism of many other substrates, including drugs and procarcinogens (see [6] for a recent review). *CYP2A6*, which is polymorphic, is mainly expressed in the liver, and it is believed to play an important role in systemic clearance of nicotine [6–9]. Genetic polymorphisms of *CYP2A6* have been linked to a reduced susceptibility to lung cancer in smokers in several studies [10–12], but not in other studies [13–15]. However, the roles of CYP2A6-mediated metabolism of xenobiotic substrates in drug clearance, chemical toxicity, and carcinogenesis have yet to be directly demonstrated in an in vivo model.

The aim of this study was to prepare and characterize a CYP2A6-transgenic mouse model, a model that should be valuable for directly demonstrating the in vivo functions of this polymorphic human enzyme in drug metabolism and chemical toxicity. An embryonic stem (ES) cell-based approach was used for transgenic mouse production. The transgene construct contained a full-length CYP2A6 cDNA, driven by the mouse transthyretin (TTR) promoter/enhancer, and a downstream neomycin-resistance gene (Neo) for positive selection in ES cells. The CYP2A6-transgenic mouse was originally generated on a mixed C57BL/6 (B6) and 129/Sv genetic background, and it was backcrossed to the B6 strain for six generations for subsequent characterization. This was necessary because the orthologous mouse *Cyp2a5* genes of the two parental mouse strains have structural and regulatory differences that would

* Corresponding author. Fax: +1 518 486 1505.
E-mail address: xding@wadsworth.org (X. Ding).
[1] Present address: Van Andel Research Institute, 333 Bostwick NE, Grand Rapids, MI 49503, USA.

0006-291X/$ - see front matter © 2005 Elsevier Inc. All rights reserved.
doi:10.1016/j.bbrc.2005.08.086

confound the analysis of the transgenic CYP2A6. Here, we present evidence for the hepatic expression of the *CYP2A6* transgene, and initial studies on the in vitro and in vivo activities of transgenic CYP2A6 toward coumarin.

Materials and methods

Construction of CYP2A6 transgene and generation of transgenic mice. The *CYP2A6* transgene (Fig. 1) was constructed in a pPGK-neo-bpA vector [16], which contained a Neo gene cassette (consisting of the mouse phosphoglycerate kinase promoter, bacterial neomycin phosphoribosyl transferase gene, and bovine growth hormone 3′-untranslated sequence with polyadenylation signal) and a pBluescript backbone. The TTR-promoter/enhancer fragment (−3.0 kb to +20 bp) [17] was inserted at the *Sal*I/*Hin*dIII sites. The coding exons and 3′-flanking sequence of CYP2A6 were obtained by RNA-PCR from human liver RNA (exons 1–9) and by genomic PCR from human genomic DNA (exon 8 and 3′-flanking region); the two PCR fragments were joined (1.85 kb) at a common *Sac*I site in exon 9, and the resulting full-length cDNA was inserted downstream of the promoter fragment at an *Eco*RI site. For CYP2A6 E1–E9 RNA-PCR, the 5′-primer was 5′-actgaattctaccaccatgctggcctcagg-3′ (with the ATG start codon underlined and an *Eco*RI site double-underlined) and the 3′-primer was 5′-tcagcggggcaggaagctcatgg-3′ (with the stop codon underlined). For E8-3′-UTR genomic PCR, the 5′-primer was 5′-gctctgtgctgagagaccc-3′ and the 3′-primer was 5′-taggaattctaa gcctcagttttgtcacg-3′ (with an *Eco*RI site double-underlined). The transgene insert (~6.5 kb) was removed from the plasmid by double digestion with *Sal*I/*Not*I, purified, and used for electroporation into ES cells. CJ7 embryonic stem cells [18], derived from the 129/Sv strain, were used for electroporation. Transgene-positive ES cells were selected for neomycin resistance and were used to produce chimeric, *CYP2A6*-positive founder mice by the Wadsworth Center Transgenic Mouse and Gene Knockout Core facility, as described recently for the production of Cpr^{low} mice [19].

Genotype analysis and mouse breeding. *CYP2A6* transgene was detected in ES cells and mouse tissues by PCR, using primers 2A6/7F2 (5′-gggccaagatgccctacatg-3′) and 2A6/7R2 (5′-cgtcaatgtccttaggtgactgg-3′), with an annealing temperature of 68 °C, and an expected product of ~370 bp. Southern blot analysis of genomic DNA was performed essentially as described previously [20], except that genomic DNA was digested with *Hin*dIII, and that the blots were incubated with the Neo insert [16], or with a 1.5-kb CYP2A13 cDNA probe [21]. Radiolabeled DNA probes were incubated with the blots at 59 °C for 2 h. The *Cyp2a5* locus of the transgenic mice was genotyped, as described recently [22], by sequencing genomic PCR products containing the Ala/Val117 polymorphic site in *Cyp2a5* exon 3 [23].

Male chimeric *CYP2A6* founder mice were bred with wild-type B6 female mice to obtain N1 mice that were hemizygous for the transgene. The N1 hemizygotes, on a mixed B6 and 129/Sv background, were used for Southern blot analysis and initial studies of transgene expression. Later, they were backcrossed to B6 mice for five more generations; the resultant N6 hemizygotes were intercrossed to obtain homozygous CYP2A6-transgenic breeding pairs. Offspring from the N6 transgenic mice were used for subsequent characterization.

Detection of CYP2A6 expression. Total RNA was isolated with use of the RNeasy Mini kit (Qiagen, Valencia, CA). RNA concentration and purity were determined spectrally. RNA-PCR was performed with a set of CYP2A6-specific primers [24]. All RNA samples were treated with DNase I (Life Technologies, Carlsbad, CA) before reverse transcription (RT). RT reactions were performed in a PE9600 PCR machine (Applied Biosystems, Foster City, CA). First-strand cDNAs were synthesized at 50 °C for 50 min, using the SuperScript III First-Strand Synthesis System (Life Technologies), with use of 1 μg total RNA, 2.5 μM oligo$(dT)_{20}$ primer, 0.5 mM dNTP mix, and 5 mM $MgCl_2$ in a total volume of 20 μl. RNA-PCR was carried out using a LightCycler instrument (Roche, Mannheim, Germany) and a LightCycler FastStart DNA Master SYBR Green I kit (Roche Applied Science, Indianapolis, IN). PCR mixtures contained 1 μl of FastStart DNA Master SYBR Green I, 3.5 mM (final concentration) $MgCl_2$, 0.3 μM each primer, and 1 μl RT product, in a total volume of 10 μl. PCR was monitored for 35 cycles with denaturation at 95 °C for 10 s, annealing at 66 °C for 5 s, and extension at 72 °C for 20 s. Purity of the PCR products was confirmed by melting-curve analysis, performed at the end of the PCR cycles, and by electrophoretic analysis on agarose gels. The CYP2A6 cDNA clone was used as a positive control, while potential contamination of reagents was monitored in negative control reactions (no template).

RNA-blot analysis was performed as described previously [25] with a full-length CYP2A6 cDNA probe (1.8 kb) or a CYP2A5 cDNA probe [26]. The sizes of the transcripts detected were estimated by comparisons with fragments of a RNA ladder. Microsomes were prepared as previously described [25]. Immunoblot analysis was performed essentially as described previously [27], but with a monoclonal antibody to CYP2A6 (Invitrogen, Carlsbad, CA); the antibody, diluted at 1:1000, was incubated with the blots at room temperature for 1 h.

Determination of coumarin and 7-hydroxycoumarin in the blood. Animal-use protocols were approved by the Institutional Animal Care and Use Committee of the Wadsworth Center. Mice were given a single i.p. dose of coumarin (in 0.1 ml dimethyl sulfoxide) at 80 mg/kg, and blood samples (~10 μl each) were collected by tail bleeding at various time points after treatment. Coumarin and 7-hydroxycoumarin were determined by HPLC, with use of authentic compounds as standards for quantification. At each time point, plasma samples from three mice were pooled as one sample, to which 1/3 vol of 20% trichloroacetic acid was added for precipitation of proteins. After centrifugation at ~15,000*g* for 15 min at 4 °C, 15 μl of the supernatant was used for HPLC analysis. Coumarin and 7-hydroxycoumarin were separated on a Waters (Milford, MA) μBondapak C18 column (3.9 × 150 mm), with an isocratic mobile phase of 70% A (20 mM triethylamine and 75 mM ammonium acetate, pH 4.0) and 30% B (methanol). The eluates were monitored at 260 nm.

Other methods. Protein concentrations were determined by the bicinchoninic acid method (Pierce, Rockford, IL) using bovine serum

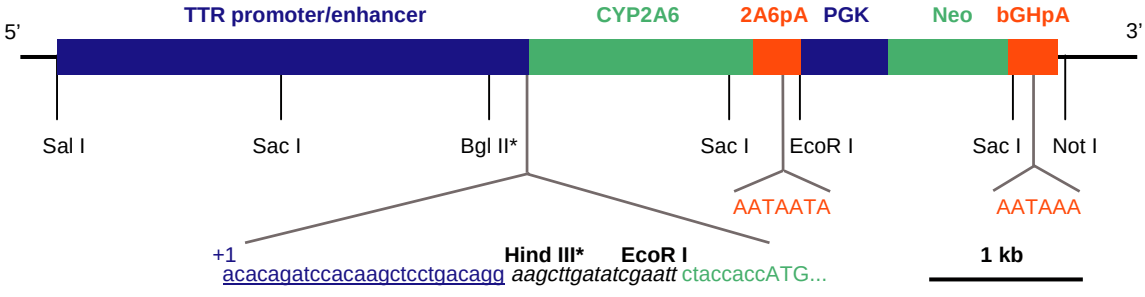

Fig. 1. Structure of the *CYP2A6* transgene. The transgene consisted of a full-length CYP2A6 cDNA (GenBank Accession No. M33318), driven by the TTR (GeneID: 22139) promoter and enhancer, and a Neo gene driven by the PGK promoter. The sequence between the cap site (+1) and the translation initiation codon (ATG) is indicated. Italicized nucleotides were from the multiple cloning region of the vectors used, and underlined nucleotides were from the 5′-untranslated region of TTR cDNA. The approximate positions of the CYP2A6 polyadenylation signal (2A6pA), and that of the bovine growth hormone (bGHpA), are also shown. *Unique restriction sites. Purified *Sal*I–*Not*I fragment was used for electroporation of ES cells.

albumin as the standard. Microsomal P450 concentration was determined by CO-difference spectroscopy [28]. Coumarin 7-hydroxylase assays were performed according to the method of Greenlee and Poland [29], with use of a model LS50B Luminescence Spectrometer (Perkin-Elmer). Coumarin and metyrapone (Sigma) were added in methanol; the amount of methanol added was less than 1% of the total reaction volume, and it was kept constant in all reactions.

Results

Generation and general characterization of CYP2A6-transgenic mice

The structure of the *CYP2A6* transgene is shown in Fig. 1. To achieve targeted liver expression of human CYP2A6, we inserted the CYP2A6 cDNA downstream of a mouse liver-specific TTR promoter/enhancer, a strategy that has been used successfully in previous studies for achieving constitutive expression of a transgene in mouse liver [30]. Because we used an ES cell-based approach for transgene introduction, which was unusual, we incorporated a neomycin-resistance gene downstream of the CYP2A6 cDNA. Following electroporation with purified *CYP2A6* transgene, and subsequent antibiotic selection, transgene-positive ES cell clones were readily identified. Chimeric mice generated with a transgene-positive ES cell clone (designated as L1) achieved germline transmission upon crossing with B6 mice.

Southern blot analysis of *Hin*dIII-digested genomic DNA from F1 hemizygous pups indicated that the integrated transgene contained both the *CYP2A6* cassette and the Neo cassette, since both a Neo probe and a CYP2A13 cDNA probe, which has a high sequence homology to the *CYP2A6* transgene (~95% sequence identity), detected the same band, ~5 kb, in the transgenic mice, but not in wild-type controls (data not shown). The result of Southern blot analysis also suggested that only one copy of the transgene was incorporated into the mouse genome in this transgenic line. This conclusion was based on the fact that only a single Neo-containing *Hin*dIII restriction fragment (~5 kb), which was smaller than the size of the full-length transgene insert (6.5 kb), was detected; the ~5-kb fragment presumably resulted from cuts at the unique *Hin*dIII site immediately upstream of the *CYP2A6* transgene coding region, and at a downstream *Hin*dIII site in the mouse genome, near the site of transgene integration.

The hemizygous CYP2A6-transgenic mice, on a 50% B6 and 50% 129/Sv genetic background, were backcrossed to B6 mice for five more generations, over a period of about 2 years. The resultant hemizygotes (N6 on the B6 background) were intercrossed to generate nearly congenic, homozygous CYP2A6-transgenic mice for characterization of transgene expression and function, as well as for maintenance of the colony. Homozygous CYP2A6-transgenic mice were indistinguishable from wild-type B6 mice in general appearance, growth rate, and reproductive ability.

Analysis of CYP2A6 transgene expression in the transgenic mice

The expression of the *CYP2A6* transgene was first analyzed by RNA-PCR, with a set of CYP2A6-specific primers that amplify a ~380-bp fragment within the coding region. As shown in Fig. 2A, a band, of the correct size, was detected, by ethidium bromide staining of PCR products, only in RNA samples of the transgenic mouse liver, but not in those from the livers of wild-type B6 mice. CYP2A6 mRNA was also not detected in other tissues examined, from either wild type (not shown) or the transgenic mice (Fig. 2): lung, kidney, small intestine, and olfactory mucosa; this result confirmed that the transgene was selectively expressed in the liver. It should be noted that, in a previous study, the TTR promoter/enhancer directed the expression of a TTR minigene in the choroid plexus, as well as in liver, in transgenic mice [30]. In the present study, we did not determine whether the *CYP2A6* transgene is expressed in the choroid plexus in the CYP2A6-transgenic mice.

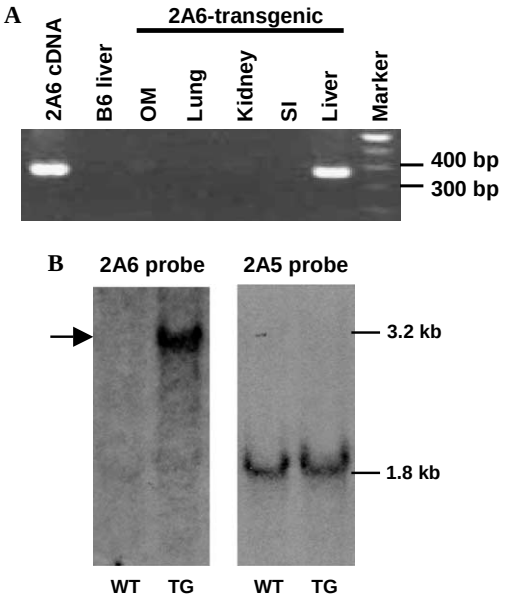

Fig. 2. Expression of the *CYP2A6* transgene. (A) RNA-PCR analysis of CYP2A6 tissue distribution. Total RNA was isolated from various tissues of B6 and homozygous CYP2A6-transgenic mice; tissues from three mice were combined in each sample. RNA-PCR detection of CYP2A6 was performed as described in Materials and methods, with use of *CYP2A6* gene-specific primers. PCR products were analyzed by electrophoresis on an agarose gel and visualized by staining with ethidium bromide. A CYP2A6 cDNA clone was used as a positive control, whereas RNA from B6 mouse liver was used as a negative control. Selected fragments of a 100-bp DNA ladder are indicated. The expected size of the CYP2A6-derived PCR product is ~380 bp. (B) Northern blot detection of transgene mRNA. Hepatic RNA samples (10 μg/lane) from hemizygous transgenic mice (TG) or wild-type littermates (WT) were analyzed on a Northern blot, with use of a ^{32}P-labeled CYP2A6 cDNA probe or a CYP2A5 cDNA probe. RNA samples from three individual mice were analyzed for each genotype, and typical results (from one mouse for each group) are shown. The approximate sizes of the transcripts detected are indicated. An arrow marks the band corresponding to the CYP2A6-Neo bicistronic RNA, detected in the transgenic mouse with the CYP2A6 probe.

Hepatic expression of the transgene was further analyzed on RNA blots, with use of a full-length CYP2A6 cDNA probe, as well as a CYP2A5 cDNA probe for detecting the mouse CYP2A transcripts (Fig. 2B). With the CYP2A6 probe, a 3.2-kb band was detected in the transgenic mouse, but not in the wild-type littermate. This transcript was longer than either the CYP2A6 transcript detected in human liver RNA (~1.8 kb; not shown) or the mouse CYP2A transcripts (also ~1.8 kb; Fig. 2B) detected in both transgenic and wild-type mice. The 3.2-kb transcript, in addition to a smaller (but more abundant) Neo transcript, was detected by a Neo cDNA probe on RNA blots (data not shown), an observation indicating that the 3.2-kb RNA was a bicistronic transcript containing the CYP2A6 cDNA and the Neo cassette. In other experiments not shown, the occurrence of the bicistronic CYP2A6-neo mRNA was further confirmed by RNA-PCR using a CYP2A6 forward primer and a Neo reverse primer. It appears that transcription of the transgene did not stop at the CYP2A6 polyadenylation signal. Instead, the downstream bovine growth hormone mRNA polyadenylation signal associated with the Neo cassette was utilized, generating a 3.2-kb bicistronic mRNA.

Hepatic expression of CYP2A6 protein was confirmed by immunoblot analysis with a monoclonal antibody to CYP2A6. As shown in Fig. 3A, a band corresponding to CYP2A6 was detected in the transgenic mouse liver microsomes, but was largely absent in the liver microsomes from B6 mice. Additional, quantitative immunoblot analysis (not shown) indicated that the level of transgenic CYP2A6 protein was ~5 pmol/mg hepatic microsomal protein or about 1% of total P450 in mouse liver microsomes. The precise level of CYP2A5 protein in liver microsomes is not known, because antibodies that can distinguish various mouse CYP2A proteins, i.e., CYP2A4, CYP2A5, CYP2A12, and possibly CYP2A22 [31], are not yet available. However, assuming that CYP2A5 is the major CYP2A protein in mouse liver microsomes, we estimate that the level of endogenous CYP2A5 protein is higher than 5 pmol/mg.

Demonstration of in vitro and in vivo activities of CYP2A6 in the transgenic mice

The enzyme activities of CYP2A6 in hepatic microsomes of CYP2A6-transgenic mice were demonstrated with coumarin as a substrate. A mouse CYP2A5 inhibitor, metyrapone, which does not significantly inhibit human CYP2A6 activity [32], was used in the assays to eliminate the endogenous CYP2A5-catalyzed coumarin 7-hydroxylase activity. As shown in Fig. 3B, hepatic microsomal coumarin 7-hydroxylase activities, determined at a near-saturating substrate concentration (100 μM), were significantly higher in the transgenic mice than in B6 mice. Addition of 500 μM metyrapone, a concentration known to inhibit >90% of CYP2A5 activity [32], nearly abolished the activity in B6 mice, but did not cause a significant inhibition of the activity in transgenic mice. The apparent lack of inhibition of microsomal coumarin hydroxylase activity seems to suggest that CYP2A5 did not contribute to hepatic microsomal coumarin hydroxylation in the transgenic mice. However, the relatively large inter-individual variations in microsomal activity among the transgenic mice, compared to the low activity seen in the B6 mice, could have obscured any contribution of CYP2A5.

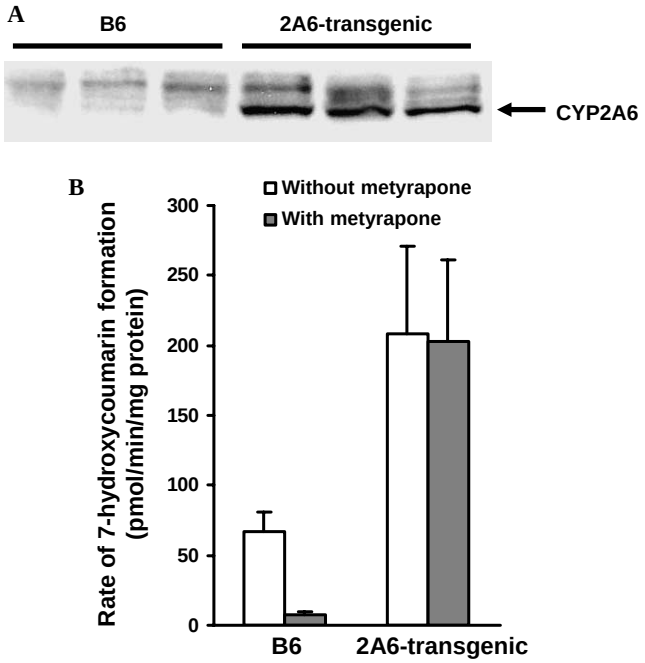

Fig. 3. Expression of functional CYP2A6 protein in transgenic mouse liver. (A) Immunoblot analysis. Microsomes pooled from three adult, male B6 mice or CYP2A6-transgenic mice (5 μg protein per lane) were analyzed on an immunoblot using a monoclonal antibody to CYP2A6. The antibody has weak cross-reaction with CYP2A5. The unique band detected in the transgenic mice (indicated by an arrow) co-migrated with a heterologously expressed CYP2A6 standard (not shown). (B) Coumarin 7-hydroxylase activity. Coumarin 7-hydroxylation assay was performed as described in the legend to Table 1, with use of 100 μM coumarin as the substrate. Metyrapone (500 μM), which inhibits mouse CYP2A5 but essentially does not inhibit human CYP2A6, caused significant inhibition of microsomal coumarin hydroxylase activity in B6 mice (Student's t test, $p < 0.01$), but not in CYP2A6-transgenic mice.

Kinetic analysis was performed to determine whether the coumarin 7-hydroxylases in liver microsomes from B6 and CYP2A6-transgenic mice differed in V_{max}, or K_m, or both. As shown in Table 1, microsomes from the transgenic mice had V_{max} values ~4 times higher than those for the B6 mice, but the two strains shared similar apparent K_m values for coumarin 7-hydroxylation. Consequently, the apparent catalytic efficiency was much higher for the transgenic mice than for B6 mice, a finding that further demonstrates the contribution of transgenic CYP2A6.

The contribution of transgenic CYP2A6 to systemic drug clearance was determined by a comparison of blood levels of coumarin and 7-hydroxycoumarin following a single i.p. injection of coumarin at 80 mg/kg. As shown in Fig. 4, coumarin was cleared within 3 h after dosing, in

Table 1
Kinetic analysis of coumarin 7-hydroxylation by liver microsomes from B6 and CYP2A6-transgenic mice

Mouse strain	V_{max} (pmol/min/mg protein)	K_m (μM)	V_{max}/K_m
B6	48 ± 6	6.9 ± 4.0	7
CYP2A6-transgenic	$226 \pm 67^*$	7.3 ± 2.5	31

Reaction mixtures contained 0.5 mg/ml microsomal protein, 50 mM phosphate buffer, pH 7.4, 1 mM NADPH, and coumarin at 1–100 μM. The reactions were carried out at 37 °C for 10 min. Microsomes were prepared from pooled liver tissues of five mice in each group (male, 3 months old). The formation of 7-hydroxycoumarin was determined as described in Materials and methods. Values presented are means ± SD of the results from three determinations.

* Significantly different from B6 control mice ($p < 0.01$).

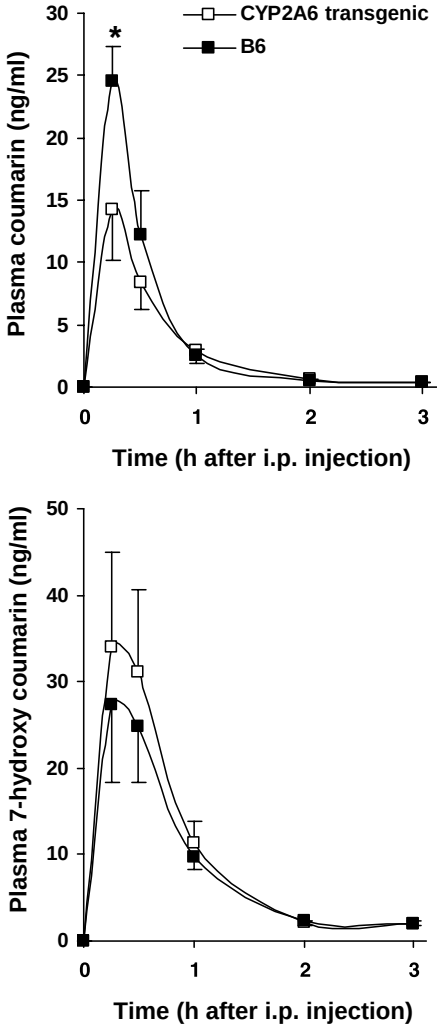

Fig. 4. In vivo metabolism of coumarin in B6 and CYP2A6-transgenic mice. Plasma levels of coumarin and 7-hydroxycoumarin were determined in 3-month-old, male B6 and CYP2A6-transgenic mice, following a single i.p. injection of coumarin at 80 mg/kg. Blood samples were collected at six time points (0, 15, and 30 min, and 1, 2, and 3 h) after the treatment; for each time point, plasma aliquots from three mice were pooled as one sample for HPLC analysis. Each datum represents the mean ± SD of three samples (from a total of nine mice). *$p < 0.05$, CYP2A6-transgenic vs. B6 mice.

both mouse strains. At 15 min after dosing, the plasma coumarin level was significantly lower ($p < 0.05$) in the transgenic mice than in B6 controls. The C_{max} values were 25 ± 3 and 14 ± 4 ng/ml for the B6 and transgenic mice, respectively. Corresponding differences (although not statistically significant) in plasma levels of 7-hydroxycoumarin were also observed, with an apparently higher level in the transgenic mice than in the B6 controls.

Discussion

Transgenic mouse models that express human CYP2A6 have not been reported previously. In this study, we have successfully generated a CYP2A6-transgenic mouse model. The transgene appeared to be expressed only in the liver, where the heterologously expressed CYP2A6 contributed significantly to the metabolism of coumarin, a known CYP2A6 substrate. Thus, this mouse model will be useful for studying the capacity of hepatic CYP2A6 to metabolize additional drugs and other xenobiotic substrates in an in vivo context. Notably, although CYP2A6 is expressed at a relatively low level (~5 pmol/mg microsomal proteins) in the livers of CYP2A6-transgenic mice, this level is within the reported range of CYP2A6 protein content in human liver microsomes (e.g. [2]). Therefore, results obtained from this mouse model could be used for predicting CYP2A6-mediated xenobiotic metabolism in human liver.

The liver-restricted expression of the CYP2A6 transgene makes the present CYP2A6-transgenic mouse model ideal for demonstrating specific contributions of hepatic CYP2A6 metabolism to xenobiotic clearance in vivo. Note, however, that, because of the apparent absence of extrahepatic transgene expression, the present mouse model should not be used for studies on the potential role of CYP2A6 in xenobiotic metabolism and toxicity in extrahepatic target tissues. In human beings, CYP2A6 is expressed in the liver, as well as in several extrahepatic tissues, particularly, tissues of the respiratory tract [33]. Therefore, future efforts to generate additional CYP2A6-transgenic mice that have CYP2A6 expression in extrahepatic tissues, perhaps with use of bacterial artificial-chromosome constructs containing the human *CYP2A6* gene, are warranted.

Efforts are currently underway to generate mice that lack endogenous *Cyp2a* genes. Although the activities of CYP2A5 can be selectively eliminated through the use of a chemical inhibitor in microsomal assays, the in vivo contributions of CYP2A5 and other mouse CYP2A enzymes are more difficult to assess, or to modulate, using a pharmacological approach. Thus, the utility of the current CYP2A6-transgenic mouse model may be limited to CYP2A6 substrates that are not efficiently metabolized by the mouse P450s, until a "humanized" CYP2A6-transgenic mouse is obtained, through crossbreeding of the present mouse model with the *Cyp2a*-null mice. In this regard, several transgenic or humanized mouse models that express human xenobiotic-metabolizing P450s have been reported (see [34] for a recent review). These mouse models offer

the exciting potential for us to gain significant insights into the role of the expressed human P450 in the in vivo metabolism of endogenous as well as xenobiotic compounds.

To achieve liver-specific expression of the *CYP2A6* transgene, we used a surrogate, liver-specific promoter/enhancer (TTP), instead of the authentic *CYP2A6* promoter, to drive the transgene expression. Consequently, the present CYP2A6-transgenic mouse model should not be used to study transcriptional regulation of the *CYP2A6* gene. In addition, the fact that the transgene is expressed as a fusion transcript containing the downstream Neo cassette also precludes the use of this model to study CYP2A6 induction through mRNA stabilization. In this regard, the apparent failure of the authentic CYP2A6 polyadenylation signal, included in the transgene construct, to terminate *CYP2A6* transcription was unexpected, and it suggests that additional 3′-flanking sequences are required for the CYP2A6 polyadenylation signal to be fully functional.

Our findings that transgenic CYP2A6 contributed significantly to coumarin metabolism in vivo, and that in vitro hepatic microsomal metabolism of coumarin was more efficient in the transgenic mice than in the B6 mice, are importants. Previous studies have shown that the 7-hydroxylation of coumarin by heterologously expressed CYP2A6 has a K_m of 2–6 μM [35,36], whereas the same reaction catalyzed by heterologously expressed CYP2A5 had a K_m of ~1 μM [37,38] or ~14 μM [35], depending on the enzyme systems used. Note, however, that the CYP2A5 cDNA used for the heterologous expression was derived from the 129/Sv strain [39,40]. Liver microsomes from the 129/Sv strain have higher V_{max} and lower K_m values than do microsomes from the B6 strain [23]. Kinetic values for coumarin metabolism by CYP2A5 of the B6 strain have not been determined. Even for the 129/Sv-derived CYP2A5, a comparison of its V_{max} value with that of CYP2A6 has not been made in a comparable system (e.g., with purified P450, and reconstituted with NADPH-P450 reductase under identical conditions); therefore, it has been difficult to determine which of the two P450s is more efficient for this reaction. Nevertheless, the present findings with the CYP2A6-transgenic mice clearly indicate that the transgenic CYP2A6 has a higher V_{max} value and a higher catalytic efficiency than does endogenous mouse CYP2A5 (of the B6 strain) in coumarin 7-hydroxylation.

Acknowledgments

The authors gratefully acknowledge the use of Wadsworth Center's Biochemistry, Molecular Genetics, and Transgenic Mouse and Gene Knockout Core facilities. We thank Drs. Laurence Kaminsky and Adriana Verschoor for reading the manuscript, and Ms. Li Zhang for technical assistance. We also thank Dr. Robert Costa of the University of Illinois at Chicago for providing the −3 kb TTR promoter/enhancer CAT plasmid. This work was supported in part by United States Public Health Service Grants ES07642 and ES013337 from the National Institute of Environmental Health Sciences, National Institutes of Health.

References

[1] M. Maurice, S. Emiliani, I. Dalet-Beluche, J. Derancourt, R. Lange, Isolation and characterization of a cytochrome P450 of the IIA subfamily from human liver microsomes, Eur. J. Biochem. 200 (1991) 511–517.
[2] C.H. Yun, T. Shimada, F.P. Guengerich, Purification and characterization of human liver microsomal cytochrome P-450 2A6, Mol. Pharmacol. 40 (1991) 679–685.
[3] O. Pelkonen, A. Rautio, H. Raunio, M. Pasanen, CYP2A6: a human coumarin 7-hydroxylase, Toxicology 144 (2000) 139–147.
[4] E.S. Messina, R.F. Tyndale, E.M. Sellers, A major role for CYP2A6 in nicotine c-oxidation by human liver microsomes, J. Pharmacol. Exp. Ther. 282 (1997) 1608–1614.
[5] H. Yamazaki, K. Inoue, M. Hashimoto, T. Shimada, Roles of CYP2A6 and CYP2B6 in nicotine C-oxidation by human liver microsomes, Arch. Toxicol. 73 (1999) 65–70.
[6] C. Xu, S. Goodz, E.A. Sellers, R.F. Tyndale, CYP2A6 genetic variation and potential consequences, Adv. Drug Deliv. Rev. 54 (2002) 1245–1256.
[7] M. Oscarson, Genetic polymorphisms in the cytochrome P450 2A6 (CYP2A6) gene: implications for interindividual differences in nicotine metabolism, Drug Metab. Dispos. 29 (2001) 91–95.
[8] H. Raunio, A. Rautio, H. Gullsten, O. Pelkonen, Polymorphisms of CYP2A6 and its practical consequences, Br. J. Clin. Pharmacol. 52 (2001) 357–363.
[9] M. Nakajima, Y. Kuroiwa, T. Yokoi, Interindividual differences in nicotine metabolism and genetic polymorphisms of human CYP2A6, Drug Metab. Rev. 34 (2002) 865–877.
[10] M. Miyamoto, Y. Umetsu, H. Dosaka-Akita, Y. Sawamura, J. Yokota, H. Kunitoh, N. Nemoto, K. Sato, N. Ariyoshi, T. Kamataki, CYP2A6 gene deletion reduces susceptibility to lung cancer, Biochem. Biophys. Res. Commun. 261 (1999) 658–660.
[11] N. Ariyoshi, M. Miyamoto, Y. Umetsu, H. Kunitoh, H. Dosaka-Akita, Y. Sawamura, J. Yokota, N. Nemoto, K. Sato, T. Kamataki, Genetic polymorphism of CYP2A6 gene and tobacco-induced lung cancer risk in male smokers, Cancer Epidemiol. Biomarkers Prev. 11 (2002) 890–894.
[12] M. Fujieda, H. Yamazaki, T. Saito, K. Kiyotani, M.A. Gyamfi, M. Sakurai, H. Dosaka-Akita, Y. Sawamura, J. Yokota, H. Kunitoh, T. Kamataki, Evaluation of CYP2A6 genetic polymorphisms as determinants of smoking behavior and tobacco-related lung cancer risk in male Japanese smokers, Carcinogenesis 25 (2004) 2451–2458.
[13] M.A. Loriot, S. Rebuissou, M. Oscarson, S. Cenee, M. Miyamoto, N. Ariyoshi, T. Kamataki, D. Hemon, P. Beaune, I. Stucker, Genetic polymorphisms of cytochrome P450 2A6 in a case-control study on lung cancer in a French population, Pharmacogenetics 11 (2001) 39–44.
[14] W. Tan, G.F. Chen, D.Y. Xing, C.Y. Song, F.F. Kadlubar, D.X. Lin, Frequency of CYP2A6 gene deletion and its relation to risk of lung and esophageal cancer in the Chinese population, Int. J. Cancer 95 (2001) 96–101.
[15] H.J. Wang, W. Tan, B.T. Hao, X.P. Miao, G.Q. Zhou, F.H. He, D.X. Lin, Substantial reduction in risk of lung adenocarcinoma associated with genetic polymorphism in CYP2A13, the most active cytochrome P450 for the metabolic activation of tobacco-specific carcinogen NNK, Cancer Res. 63 (2003) 8057–8061.
[16] P. Soriano, C. Montgomery, R. Geske, A. Bradley, Targeted disruption of the c-src proto-oncogene leads to osteopetrosis in mice, Cell 64 (1991) 693–702.
[17] R.H. Costa, E. Lai, J.E. Darnell Jr., Transcriptional control of the mouse prealbumin (transthyretin) gene: both promoter sequences and a distinct enhancer are cell specific, Mol. Cell. Biol. 6 (1986) 4697–4708.

[18] P.J. Swiatek, T. Gridley, Perinatal lethality and defects in hindbrain development in mice homozygous for a targeted mutation of the zinc finger gene Krox20, Genes Dev. 7 (1993) 2071–2084.
[19] L. Wu, J. Gu, H.D. Cui, Q.-Y. Zhang, M. Behr, C. Fang, Y. Weng, K. Kluetzman, P.J. Swiatek, W.Z. Yang, L. Kaminsky, X. Ding, Transgenic mice with a hypomorphic NADPH-Cytochrome P450 reductase gene: effects on development, reproduction, and microsomal cytochrome P450, J. Pharmacol. Exp. Ther. 312 (2005) 35–43.
[20] T. Su, Q.-Y. Zhang, J.H. Zhang, P. Swiatek, X. Ding, Expression of the rat CYP2A3 gene in transgenic mice, Drug Metab. Dispos. 30 (2002) 548–552.
[21] T. Su, Z.P. Bao, Q.-Y. Zhang, T.J. Smith, J.Y. Hong, X. Ding, Human cytochrome P450 CYP2A13: predominant expression in the respiratory tract and its high efficiency metabolic activation of a tobacco-specific carcinogen, 4-(methylnitrosamino)-1-(3-pyridyl)-1-butanone, Cancer Res. 60 (2000) 5074–5079.
[22] X.L. Zhuo, J. Gu, M.J. Behr, P.J. Swiatek, H.D. Cui, Q.-Y. Zhang, Y.Q. Xie, D.N. Collins, X. Ding, Targeted disruption of the olfactory mucosa-specific Cyp2g1 gene: impact on acetaminophen toxicity in the lateral nasal gland, and tissue-selective effects on Cyp2a5 expression, J. Pharmacol. Exp. Ther. 308 (2004) 719–728.
[23] R.L. Lindberg, R. Juvonen, M. Negishi, Molecular characterization of the murine Coh locus: an amino acid difference at position 117 confers high and low coumarin 7-hydroxylase activity in P450coh, Pharmacogenetics 2 (1992) 32–37.
[24] Y. Chen, Y.Q. Liu, T. Su, X. Ren, L. Shi, D.Z. Liu, J. Gu, Q.-Y. Zhang, X. Ding, Immunoblot analysis and immunohistochemical characterization of CYP2A expression in human olfactory mucosa, Biochem. Pharmacol. 66 (2003) 1245–1251.
[25] T. Su, J.J. Sheng, T.W. Lipinskas, X. Ding, Expression of CYP2A genes in rodent and human nasal mucosa, Drug Metab. Dispos. 24 (1996) 884–890.
[26] T. Su, W.L. He, J. Gu, T.W. Lipinskas, X. Ding, Differential xenobiotic induction of CYP2A5 in mouse liver, kidney, lung, and olfactory mucosa, Drug Metab. Dispos. 26 (1998) 822–824.
[27] J. Gu, Q.-Y. Zhang, M.B. Genter, T.W. Lipinskas, M. Negishi, D.W. Nebert, X. Ding, Purification and characterization of heterologously expressed mouse CYP2A5 and CYP2G1—role in metabolic activation of acetaminophen and 2,6-dichlorobenzonitrile in mouse olfactory mucosal microsomes, J. Pharmacol. Exp. Ther. 285 (1998) 1287–1295.
[28] T. Omura, R. Sato, The carbon monoxide-binding pigment of liver microsomes. I. Evidence for its hemoprotein nature, J. Biol. Chem. 239 (1964) 2370–2378.
[29] W.F. Greenlee, A. Poland, An improved assay of 7-ethoxycoumarin *O*-deethylase activity: induction of hepatic enzyme activity in C57BL/6J and DBA/2J mice by phenobarbital, 3-methylcholanthrene and 2,3,7,8-tetrachlorodibenzo-*p*-dioxin, J. Pharmacol. Exp. Ther. 205 (1978) 596–605.
[30] C. Yan, R.H. Costa, J.E. Darnell Jr., J.D. Chen, T.A. Van Dyke, Distinct positive and negative elements control the limited hepatocyte and choroid plexus expression of transthyretin in transgenic mice, EMBO J. 9 (1990) 869–878.
[31] H.Y. Wang, K.M. Donley, D.S. Keeney, S.M.G. Hoffman, Organization and evolution of the Cyp2 gene cluster on mouse chromosome 7, and comparison with the syntenic human cluster, Environ. Health Perspect. 111 (2003) 1835–1842.
[32] J. Maenpaa, H. Sigusch, H. Raunio, T. Syngelma, P. Vuorela, H. Vuorela, O. Pelkonen, Differential inhibition of coumarin 7-hydroxylase activity in mouse and human liver microsomes, Biochem. Pharmacol. 45 (1993) 1035–1042.
[33] T. Su, X. Ding, Regulation of the cytochrome P450 2A genes, Toxicol. Appl. Pharmacol. 199 (2004) 285–294.
[34] F.J. Gonzalez, Cytochrome P450 humanised mice, Hum. Genomics 1 (2004) 300–306.
[35] X.L. Zhuo, J. Gu, Q.-Y. Zhang, D.C. Spink, L.S. Kaminsky, X. Ding, Biotransformation of coumarin by rodent and human cytochromes P-450: metabolic basis of tissue-selective toxicity in olfactory mucosa of rats and mice, J. Pharmacol. Exp. Ther. 288 (1999) 463–471.
[36] X.Y. He, J. Shen, W.Y. Hu, X. Ding, A.Y.H. Lu, J.Y. Hong, Identification of Val(117) and Arg(372) as critical amino acid residues for the activity difference between human CYP2A6 and CYP2A13 in coumarin 7-hydroxylation, Arch. Biochem. Biophys. 427 (2004) 143–153.
[37] R. Lindberg, B. Burkhart, T. Ichikawa, M. Negishi, The structure and characterization of type I P-450(15) alpha gene as major steroid 15 alpha-hydroxylase and its comparison with type II P-450(15) alpha gene, J. Biol. Chem. 264 (1989) 6465–6471.
[38] N.D. Felicia, G.K. Rekha, S.E. Murphy, Characterization of cytochrome P450 2A4 and 2A5-catalyzed 4-(methylnitrosamino)-1-(3-pyridyl)-1-butanone (NNK) metabolism, Arch. Biochem. Biophys. 384 (2000) 418–424.
[39] E.J. Squires, M. Negishi, Reciprocal regulation of sex-dependent expression of testosterone 15 alpha-hydroxylase (P-450(15 alpha)) in liver and kidney of male mice by androgen: evidence for a single gene, J. Biol. Chem. 263 (1988) 4166–4171.
[40] R.L. Lindberg, M. Negishi, Alteration of mouse cytochrome P450coh substrate specificity by mutation of a single amino-acid residue, Nature 339 (1989) 632–634.